

Shell-Model Interpretation of the Collective-Model Potential-Energy Surface

J. P. Draayer and S. C. Park

Department of Physics and Astronomy, Louisiana State University, Baton Rouge, Louisiana 70803-4001

O. Castaños

*Instituto de Ciencias Nucleares, Universidad Nacional Autónoma de México,
Apartado Postal 70-543, México, D.F. 01000, México*

(Received 3 October 1988)

The potential-energy-surface concept of the generalized collective model is given a shell-model interpretation. For deformation less than the equilibrium value, $\beta < \beta_0$, the shape of the potential is related to intrashell dynamics while the sharp rise for $\beta > \beta_0$ is shown to be an intershell phenomenon that depends on competition between major shell excitation energies and the binding energy of the residual interaction. The exclusion principle plays an essential role in the argument. Results for ^{24}Mg illustrate the necessity of an open-shell picture.

PACS numbers: 21.60.Ev, 21.60.Cs, 21.60.Fw, 27.30.+t

The purpose of this Letter is to give a shell-model interpretation of the potential-energy-surface (PES) concept of the Gneuss-Greiner model (GGM).¹ The latter is a phenomenological theory that describes nuclei in terms of collective quadrupole bosons that represent shape oscillations. This objective will be met within the framework of the microscopic collective model (MCM) which is an algebraic theory that has the dynamical group of the three-dimensional oscillator as its fundamental symmetry.² It is a fermion-based shell-model theory that includes intershell mixing phenomena generated by the nucleons interacting through their quadrupole fields. The MCM can be thought of as a multishell generalization of the Elliott model.³

Specifically, a simple Hamiltonian consisting of the isotropic harmonic oscillator and the collective quadrupole-quadrupole interaction is shown to suffice for the explanation of the general features of the collective-model potential. This result, together with the relation between the microscopic quadrupole operator and the collective quadrupole variables, implies that the high-order terms that enter into collective-model theories of nuclear structure serve to mimic exclusion-principle effects. If a residual rotorlike term is added to the harmonic-oscillator plus quadrupole-quadrupole interaction, low-lying spectral features like the K -band splitting can also be explained. Calculated results for the excitation spectra and $E2$ transition rates of ^{24}Mg are given to illustrate the theory.

The GGM gives a description of nuclear properties in terms of collective coordinates $\alpha_{2,\mu} \equiv a_\mu$ that define quadrupole deformations of the surface,

$$R(\theta, \phi) = R_0 \left[1 + \sum_{\mu} \alpha_{2,\mu}^* Y_{2,\mu}(\theta, \phi) \right], \quad (1)$$

and the corresponding conjugate momenta $\pi_{2,\mu} \equiv \pi_\mu$, where in a quantized picture $[\pi_\mu, \alpha_\nu] = -i\hbar \delta_{\mu\nu}$. Specifically, the Hamiltonian consists of kinetic and potential

parts built out of scalars in the collective coordinates,

$$H = T + V \text{ where } V = \sum_{\rho, \sigma} V_{\rho\sigma} \beta^{2\rho+3\sigma} (\cos 3\gamma)^\sigma. \quad (2)$$

This Hamiltonian is diagonalized in a five-dimensional harmonic-oscillator basis with $N \leq N_{\max}$ bosons. The parameters of the Hamiltonian, given in (2) in principal-axes form ($a_{2,0} = \beta \cos \gamma$, $a_{2,\pm 1} = 0$, $a_{2,\pm 2} = 1/\sqrt{2} \beta \sin \gamma$), are determined through a least-squares-fitting procedure. Gneuss and Griener used a sixth-order theory ($2\rho + 3\sigma \leq 6$) with $N_{\max} \leq 32$. An extension adds deformation-dependent terms to T and nonpolynomial parts to V .⁴ A plot of the resultant V as a function of β and γ is the PES of the GGM. The theory embodies all special cases of the collective model: the rotor, triaxial as well as symmetric, the quantum vibrator, and the so-called rotor-vibrator limit.⁵

Terms in V in order 4 (6) or greater in β are required to obtain a nonzero equilibrium β_0 (γ_0) deformation value. Furthermore, it is clear that if V_{01} enters with a negative sign there must be a positive V_{20} or V_{02} to balance it so the potential does not go to negative infinity for large β , etc. In other words, all the familiar problems encountered whenever polynomial expansions are used enter in the theory. One purpose of this Letter is to point out that these high-order terms are necessary because the GGM does not address the particle dynamics properly. Specifically, it ignores the elementary but important fact that nuclei are made up of fermions that obey the exclusion principle. Another complementary purpose is to show that stable nonzero equilibrium values for the deformation arise naturally within the framework of the shell model with no more than two-body interactions.

Consider the following simple shell-model Hamiltonian:

$$H = H_0 - \frac{1}{2} \chi Q^c \wedge Q^c, \quad (3)$$

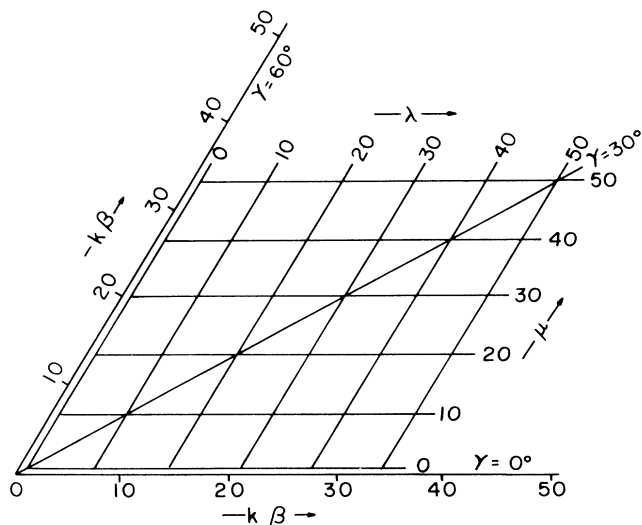


FIG. 1. A traditional (β, γ) or polar plot, with β the radius vector and γ the azimuthal angle, which shows the relationship between the collective-model shape variables (β, γ) and the $SU(3)$ irrep labels (λ, μ) .

where H_0 is the three-dimensional isotropic harmonic oscillator and $Q^c \wedge Q^c$ is the collective quadrupole-quadrupole interaction. The latter builds coherence into calculated eigenstates so they yield enhanced $E2$ transition rates. The strength of H_0 is fixed by $\hbar\omega$, the major-shell separation distance. The operator Q^c couples shells that differ by $\pm 2\hbar\omega$ and is a generator of the noncompact group $Sp(6, R)$. If the action of Q^c is restricted to the valence shell, $SU(3)$ is a good symmetry. However, the full Hamiltonian (3) has $Sp(6, R)$ as its dynamical symmetry group. The $Sp(6, R) \rightarrow SU(3) \rightarrow SO(3)$ group structure defines the MCM. It is the Elliott $SU(3)$ model extended to incorporate the inter-shell couplings generated by Q^c . The $SU(3)$ tensor character of the non- $SU(3)$ -conserving, $2\hbar\omega$ raising and lowering parts of Q^c are $(2, 0)$ and $(0, 2)$, respectively. Because shells above (below) the valence one are essentially empty (full), these raising (lowering) operators can be replaced to high accuracy by $(l=0$ and $2)$ boson creation (annihilation) operators with the same $SU(3)$ tensor character. This yields a contraction of MCM known as the $U_b(6) \times U_s(3)$ or $U(3)$ boson model.⁶

Before we present results of calculations, it is necessary to establish a connection between the shape variables β and γ of the collective model and the irreducible representation (irrep) labels λ and μ of $SU(3)$. In a recent paper this was done by the invoking of a linear mapping between the eigenvalues of the invariant operators of the rotor [$\text{tr}(Q^c)^2 = k^2\beta^2$ and $\text{tr}(Q^c)^3 = (k^3/\sqrt{6})\beta^3 \times \cos 3\gamma$ where $k^2 = \frac{5}{6}\pi A\langle r \rangle^2$] and the second- and third-order Casimir invariants of $SU(3)$.⁷ A simple justification for this can be offered: The invariant measures of two theories used to describe the same quantum

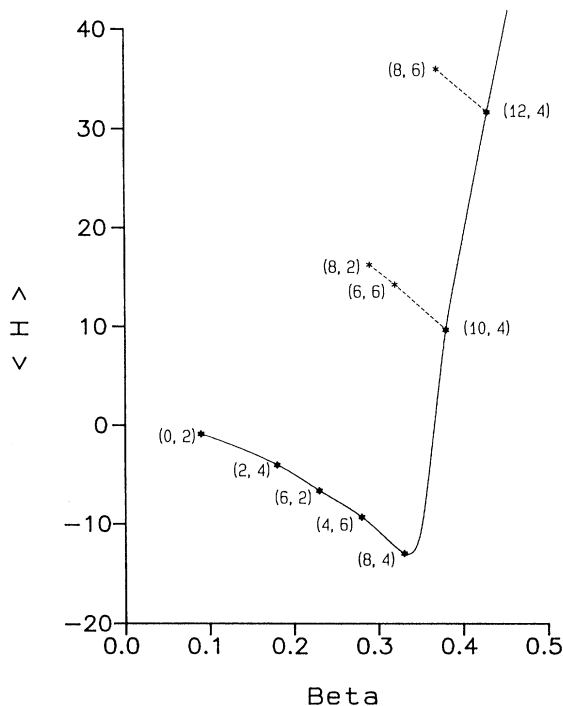


FIG. 2. Expectation value of H in $L=0$ states for the indicated irrep's of ^{24}Mg . The curve cuts through the PES with $\gamma=20.6^\circ$ for the $(8, 4)$ irrep.

phenomena must agree. The relationship is

$$\beta^2 = (4\pi/5)(A\langle r^2 \rangle)^{-2}(\lambda^2 + \lambda\mu + \mu^2 + 3\lambda + 3\mu + 3), \quad (4)$$

$$\gamma = \arctan \left[\frac{\sqrt{3}(\mu + 1)}{2\lambda + \mu + 3} \right],$$

where A is the total number of nucleons and $\langle r^2 \rangle$ is the nuclear mean square radius. In this way each (λ, μ) irrep is associated with a specific point in the (β, γ) plane. A schematic diagram that illustrates the mapping is given in Fig. 1.

The $0\hbar\omega$ $SU(3)$ irrep's for ^{24}Mg are $(0s)^4(1p)^{12}-(ds)^8$ particle configurations. They are determined by a $U(6) \rightarrow SU(3)$ group plethysm.⁸ For example, the most symmetric spatial symmetry $[f] = [444444]$ contains the following $SU(3)$ irrep's with $L=0$ states: $(\lambda, \mu) = (8, 4), (4, 6), (0, 8), (6, 2)^2, (2, 4)^2, (4, 0)^2$ and $(0, 2)$ where the superscript is a multiplicity label. Of all the allowed irrep's, including those in less symmetric spatial symmetries, the $(8, 4)$ yields the maximum value for β and for this $SU(3)$ irrep $\gamma=20.6^\circ$.

The expectation value of H ($\hbar\omega=12.6$ MeV and $\chi=0.0438$ MeV) between basis states of the $U_b(6) \times U_s(3)$ model are plotted as a function of β in Fig. 2. The solid curve traces out the locus of minimum expectation values in the $0\hbar\omega$ space for $\beta < \beta_0$ and connects leading irrep's of the $2\hbar\omega, 4\hbar\omega$, etc., spaces in the prod-

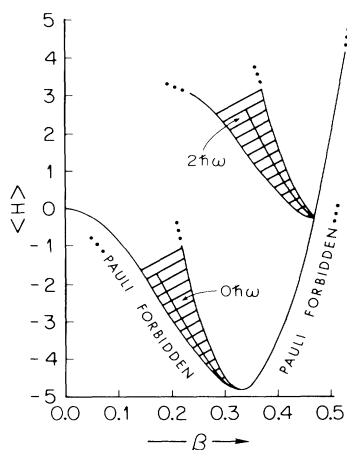


FIG. 3. A schematic diagram illustrating a shell-model realization of the collective-model PES for ^{24}Mg . In each major shell the allowed representations fall in a conical strip or V-shaped band with terminus defined by the SU(3) irrep that gives the maximum deformation in that shell. The PES corresponds to the envelope defined for $\beta < \beta_0$ by the irrep's of the $0\hbar\omega$ shell that lie lowest in energy and for $\beta > \beta_0$ by leading SU(3) irrep's of the higher shells.

ucts $(2,0)^n \times (8,4)$ for $\beta > \beta_0$. The γ values range from 46.1° for the $(0,2)$ irrep, to 20.6° for the $(8,4)$, and to 15.6° for the $(12,4)$. A point to be noted is that the slow rise to the left of the minimum ($\beta < \beta_0$) is a $0\hbar\omega$ phenomena while the sharp rise beyond the minimum ($\beta > \beta_0$) is primarily due to the shell structure. SU(3) irrep's with $\beta > \beta_0$ only exist in higher shells. If χ is set to zero, all irrep's of the n th shell would lie at $n\hbar\omega$. The actual position of the irrep's is lower than this because $Q^c \wedge Q^c$ increases the binding energy of the system. The strength of $Q^c \wedge Q^c$ must be large enough to build in the required coherence yet small enough so the shell structure established by H_0 is not destroyed. A trivial divergence can be overcome by our removing from $Q^c \wedge Q^c$ its major-shell, trace-equivalent part.⁹ This was done in the calculation.

A general microscopic (shell-model) interpretation of the macroscopic (collective-model) PES concept can now be given. A schematic plot of the expectation value of the Hamiltonian, $\langle H \rangle$, versus the deformation, β , that indicates the process is given in Fig. 3. In each major shell the allowed SU(3) representations fall into a conical band with terminus defined by the leading SU(3) irrep, that is, the (λ, μ) for which β was given by (4) is a maximum. The PES corresponds to the envelope that is defined for $\beta < \beta_0$ by the irrep's of the $0\hbar\omega$ shell that lie lowest in energy and for $\beta > \beta_0$ by leading SU(3) irrep's of the higher shells. Of course, SU(3) is not an exact symmetry so (λ, μ) mixing occurs both within and among the shells. This mixing blurs the boundaries but so long as SU(3) is a reasonably good symmetry the argument applies. Regions below and to the left (right) of

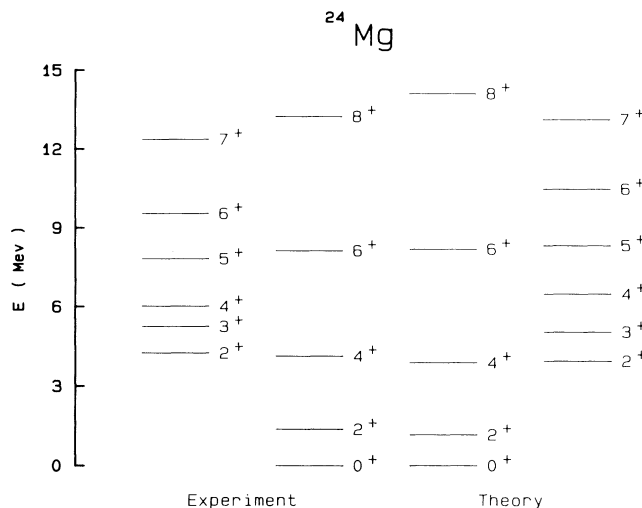


FIG. 4. Experimental and calculated $[U_b(6) \times U_s(3)]$ spectra for ^{24}Mg . Parameters of the Hamiltonian are $\hbar\omega = 12.6$ and $\chi = 0.0438$ for the shell and quadrupole-quadrupole terms, respectively, and $a = 0.130$, $b = -0.0408$, and $c = -0.00521$ for the residual SU(3) parts. All quantities are given in MeV units.

the enveloping curve for $\beta < \beta_0$ ($\beta > \beta_0$) are forbidden domains due to the Pauli principle. The equilibrium value for the deformation β_0 is determined by a complicated convolution of intrashell and intershell dynamics.

The calculated spectra for ^{24}Mg is compared with experiment in Fig. 4 and an analysis of the corresponding eigenstates is given in Table I. These results were obtained for the Hamiltonian of (3) augmented with a residual rotorlike SU(3) term that allowed the interaction to be fine tuned to reproduce the observed low-energy K-band splitting,¹⁰

$$H = H_0 - \frac{1}{2} \chi Q^c \wedge Q^c + aL^2 + bX_3 + cX_4. \quad (5)$$

In (5) the operators X_a are rotational scalars built from the generators of SU(3): $X_3 = (L \times Q \times L)^0$ and $X_4 = [(L \times Q)^1 \times (Q \times L)^1]^0$. In these expressions Q is the part of Q^c that acts within a single shell. The X_a

TABLE I. Eigenstate intensity analysis for members of the ^{24}Mg ground band.

Shell ($\hbar\omega$)	Angular momentum				
	0	2	4	6	8
0	61.1	61.4	62.0	65.4	70.3
2	23.9	23.7	23.3	21.6	18.8
4	10.9	10.8	10.6	9.5	8.2
Higher	4.1	4.1	4.1	3.5	2.7

TABLE II. Experimental and calculated $E2$ transition strengths in ^{24}Mg .

L_i	L_f	Sp(6,R)	$U_b(6) \times U_s(3)$	Experiment
2 ₁	0 ₁	20.3	21.0	20.5 ± 0.6
4 ₁	2 ₁	26.9	27.9	23 ± 4
6 ₁	4 ₁	25.6	26.6	34 ± 3^6
8 ₁	6 ₁	20.5	21.5	16 ± 6^5
4 ₂	2 ₂	10.8	11.1	16 ± 3
5 ₁	3 ₁	16.3	16.8	28 ± 5
6 ₂	4 ₂	17.7	18.0	23 ± 3^3
7 ₁	5 ₁		18.5	
8 ₂	6 ₂	14.8	14.4	> 3
2 ₂	0 ₁	1.3	1.6	1.4 ± 0.3
4 ₂	2 ₁	0.8	0.9	1.0 ± 0.2
6 ₂	4 ₁	0.8	0.8	0.8 ± 0.3^8
8 ₂	6 ₁		1.1	

operators are members of the $SU(3) \rightarrow SO(3)$ integrity basis and like L^2 have zero matrix elements in $L=0$ states so the addition of this $SU(3)$ term to the Hamiltonian does not change the arguments given regarding the PES. Interband as well as intraband transition rates were calculated and found to be in excellent agreement with experiment and full Sp(6,R) calculations (see Table II).^{11,12} No effective charge was needed. As the intraband transitions are 10 to 20 times stronger than the interband ones, this is a sensitive test to the theory.

In conclusion, the results show that the sharp rise in the PES for $\beta > \beta_0$ is a shell-model feature that can be reproduced with a simple two-body interaction. The GGM requires high-order terms in the potential to get stable nonzero equilibrium deformation values because there is no other mechanism for building the exclusion principle into the theory. The importance of the shell admixtures in low-lying eigenstates is signaled by enhanced $E2$ transition strengths. Typically, in low-lying eigenstates the summed intensities of shell admixed configurations is between 30% and 40%. This percentage is much too large to be ignored in any microscopic theory of nuclear structure.

This work was supported in part by the Consejo Nacional de Ciencia y Tecnología and the U.S. National

Science Foundation, including support under the U.S.-México Cooperative Science Program.

¹G. Gneuss and W. Greiner, Nucl. Phys. A **171**, 449 (1971).

²D. J. Rowe, Rep. Prog. Phys. **48**, 1419 (1985).

³J. P. Elliott, Proc. Roy. Soc. London A **245**, 128, 562 (1981).

⁴P. O. Hess, J. Maruhn, and W. Greiner, J. Phys. G **7**, 737 (1981).

⁵A. Faessler, W. Greiner, and R. K. Sheline, Nucl. Phys. **70**, 33 (1965); A. S. Davydov and G. F. Fillipov, Nucl. Phys. **8**, 237 (1958).

⁶O. Castaños and J. P. Draayer, to be published; D. J. Rowe and G. Rosensteel, Phys. Rev. C **25**, 3236 (1982).

⁷O. Castaños, J. P. Draayer, and Y. Leschber, Z. Phys. A **329**, 33 (1988).

⁸R. Pérez and J. Flores, Nucl. Data Sect. A **4**, 265 (1968).

⁹G. Rosensteel and J. P. Draayer, Nucl. Phys. A **436**, 445 (1985).

¹⁰Y. Leschber, J. P. Draayer, and G. Rosensteel, J. Phys. G **12**, L179 (1986).

¹¹G. Rosensteel, J. P. Draayer, and K. J. Weeks, Nucl. Phys. A **419**, 1 (1984).

¹²J. Keinonen, P. Tikkanen, A. Kuronen, A. Kiss, E. Somorjai, and B. H. Wildenthal, "Short Lifetimes in ^{24}Mg " (to be published).